

Metallic Graphene Nanodisks

Motohiko Ezawa

Department of Physics, University of Tokyo, Hongo 7-3-1, 113-0033, Japan

We explore the electronic properties of finite-length graphene nanoribbons as well as graphene nanodisks with various sizes and shapes in quest of metallic ones. For this purpose it is sufficient to search zero-energy states. We find that there exist no zero-energy states in finite-length zigzag nanoribbons though all infinite-length zigzag nanoribbons have zero-energy states. The occurrence of zero-energy states is surprisingly rare. Among typical nanodisks, only trigonal zigzag nanodisks have degenerate zero-energy states and show metallic ferromagnetism, where the degeneracy can be controlled arbitrarily by designing the size. A remarkable property is that the relaxation time is quite large in spite of its small size in trigonal zigzag nanodisks.

I. INTRODUCTION

Graphene^{1,2,3}, a single atomic layer of graphite, has invoked a great interest in the electronic properties of graphene-related materials. In particular, graphene nanoribbons^{4,5,6,7,8,9,10,11,12} have attracted much attention due to a rich variety of band gaps, from metals to wide-gap semiconductors. They are manufactured by patterning based on nanoelectronic lithography methods^{10,11,13}. It is interesting that graphene with a zigzag edge has the half-filled flat band at the zero-energy level and show edge ferromagnetism⁴. The half-filled zero-energy states emerge also in all zigzag nanoribbons and hence they are metallic^{4,5}. However, realistic nanoribbons have finite length. It is important to investigate the finite-length effects on the electronic properties of nanoribbons.

Another basic element of graphene derivatives is a graphene nanodisk¹⁴. It is a nanometer-scale disk-like material which has a closed edge. A graphene nanodisk can be constructed by connecting several benzenes. There are many type of nanodisks, where typical examples are displayed in Fig.1. Finite-length nanoribbons may be regarded as nanodisks provided that their length is short [Fig.2]. Some of nanodisks have already been manufactured by soft-landing mass spectrometry¹⁵.

In this paper we analyze the electric properties of nanodisks as well as finite-length nanoribbons. Since all zigzag nanoribbons are metallic, as we have mentioned, we expect all zigzag graphene derivatives are also metallic. On the contrary, the emergence of zero-energy states is quite rare. We show that there are no zero-energy states in finite-length zigzag nanoribbons. We also investigate a class of trigonal and hexagonal nanodisks possessing zigzag or armchair edges, among which we have found zero-energy states only in trigonal zigzag nanodisks.

Trigonal zigzag nanodisks are prominent in their electronic properties because there exist half-filled zero-energy states and they are metallic. Indeed, we can engineer nanodisks equipped with an arbitrary number of degenerate zero-energy states. Furthermore, spins are argued to make a ferromagnetic coupling. A remarkable property is that the relaxation time is quite large in spite

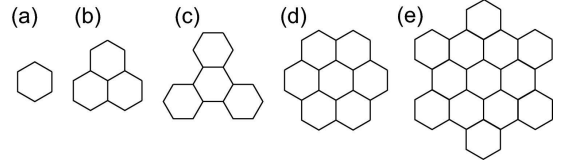


FIG. 1: Basic configurations of typical graphene nanodisks. (a) Benzene. (b) Trigonal zigzag nanodisk (phenalene). (c) Trigonal armchair nanodisk (triphenylene). (d) Hexagonal zigzag nanodisk (coronene). (e) Hexagonal armchair nanodisk (hexa benzocoronene)¹⁵.

of its small size.

This paper is organized as follows. In Section II and III, based on the tight-binding Hamiltonian, we calculate the energy spectra of finite-length zigzag nanoribbons and of a wide class of graphene nanodisks, respectively. In Section III, we also carry out a systematic investigation of the zero energy states in trigonal zigzag nanodisks. In Section IV, we analyze the wave functions of these zero-energy states to examine how they are localized at the edges. In Section V, we study the spin-relaxation time of nanodisks. Section VI is devoted to discussions.

II. ENERGY SPECTRUM OF FINITE-LENGTH NANORIBBONS

We calculate the energy spectra of graphene derivatives based on the nearest-neighbor tight-binding model, which has been successfully applied to the studies of carbon nanotubes¹⁶ and nanoribbons⁵. The Hamiltonian is defined by

$$H = \sum_i \varepsilon_i c_i^\dagger c_i + \sum_{\langle i,j \rangle} t_{ij} c_i^\dagger c_j, \quad (2.1)$$

where ε_i is the site energy, t_{ij} is the transfer energy, and c_i^\dagger is the creation operator of the π electron at the site i . The summation is taken over all nearest neighboring sites $\langle i, j \rangle$. Owing to their homogeneous geometrical configuration, we may take constant values for these energies, $\varepsilon_i = \varepsilon_F$ and $t_{ij} = t$. Then, the diagonal term in (2.1)

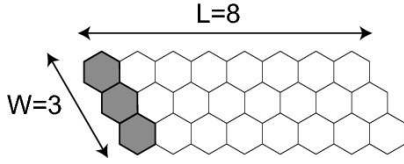


FIG. 2: Geometric configuration of zigzag nanoribbons with width W and length L . Here we show the example of the $(W, L) = (3, 8)$ nanoribbon. The basic chain is W connected benzene depicted in gray. Short nanoribbons may be regarded as parallelogrammic nanodisks.

yields just a constant, $\varepsilon_F N_C$, where N_C is the number of carbon atoms in the system. The Hamiltonian (2.1) yields the Dirac electrons for graphene^{1,2,3}. There exists one electron per one carbon and the band-filling factor is $1/2$. It is customary to choose the zero-energy level of the tight-binding Hamiltonian (2.1) at this point so that the energy spectrum is symmetric between the positive and negative energy states. Therefore, the system is metallic provided that there exists zero-energy states in the spectrum.

In this section we investigate finite-length nanoribbons to know if there are zero-energy states. A classification of infinite-length nanoribbons is given in a previous work⁵. Here we concentrate on finite-length zigzag nanoribbons. We classify them as follows (Fig.2). First we take a basic chain of W connected carbon hexagons, as depicted in dark gray. Second we translate this chain. Repeating this translation L times we construct a nanoribbon indexed by a set of two integers (W, L) . In what follows we analyze a class of finite-length nanoribbons generated in this way. Parameters W and L specify the width and the length of nanoribbons, respectively. The infinite-length nanoribbons are obtained by letting $L \rightarrow \infty$. The finite-length nanoribbons are regarded as parallelogrammic nanodisks when $L \approx W$.

In analyzing a nanoribbon containing N_C carbon atoms, the Hamiltonian (2.1) is reduced to an $N_C \times N_C$ matrix. It is possible to diagonalize the Hamiltonian exactly to determine the energy spectrum E_i together with its degeneracy g_i for each finite-length nanoribbon. The density of state is given by

$$D(\varepsilon) = \sum_{i=1}^{N_C} g_i \delta(\varepsilon - E_i). \quad (2.2)$$

It can be shown that the determinant associated with the Hamiltonian (2.1) has a factor such that

$$\det[\varepsilon I - H(N_C)] \propto (\varepsilon - t)^{a(W,L)} (\varepsilon + t)^{a(W,L)}, \quad (2.3)$$

implying the $a(W, L)$ -fold degeneracy of the states with

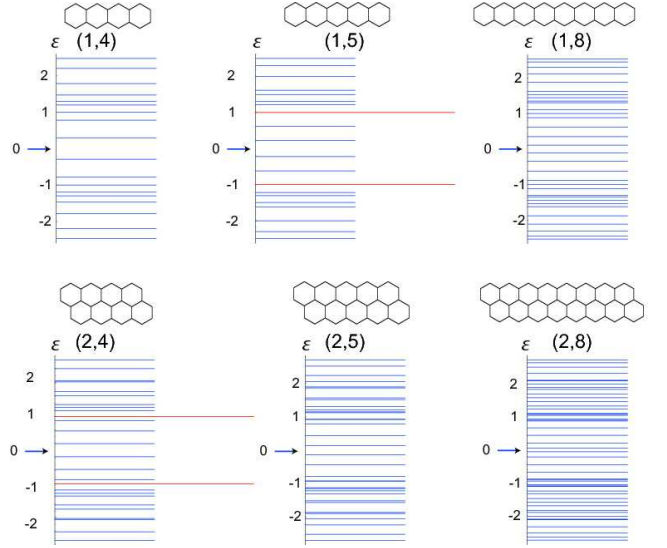


FIG. 3: (Color online) Density of states of finite-length nanoribbons. The vertical axes is the energy ε in units of $t = 3\text{eV}$, and the horizontal axes is the degeneracy. There exist no zero-energy states.

the energy $\varepsilon = \pm t$, where

$$a(1, L) = 2, 1, 2, 1, 2, 1, 2, 1, \dots, \quad (2.4a)$$

$$a(2, L) = 1, 1, 0, 2, 0, 1, 1, 0, 2, 0, \dots, \quad (2.4b)$$

$$a(3, L) = 2, 0, 2, 0, 2, 0, 2, 0, \dots, \quad (2.4c)$$

$$a(4, L) = 1, 2, 0, 3, 0, 2, 1, 1, 2, 0, \dots \quad (2.4d)$$

We have displayed the full spectra for some examples of finite-length nanoribbons by taking $t = 3\text{eV}$ in Fig.3.

One of our main results is that there are no zero-energy states in finite-length nanoribbons. However, the band gap decreases inversely to the length, and zero-energy states emerge as $L \rightarrow \infty$, as shown in Fig.4. This is consistent with the fact that infinite-length nanoribbons have the flat band made of degenerated zero-energy states^{4,5}. Hence, a sufficiently long nanoribbon can be regarded practically as a metal.

III. ENERGY SPECTRUM OF NANODISKS

We next derive the energy spectrum of each nanodisk [Fig.1] by diagonalizing the Hamiltonian (2.1). As an example we display the density of state (2.2) of trigonal zigzag nanodisks in Fig.5. We have classified them by the size parameter N as defined in Fig.5(a). The number of carbons are given by $N_C = N^2 + 6N + 6$.

In order to reveal a global structure, it is convenient to introduce the doped electron number at a given energy E , which we normalize as

$$n(E) = \frac{1}{N_C} \int_0^E D(\varepsilon) d\varepsilon, \quad (3.1)$$

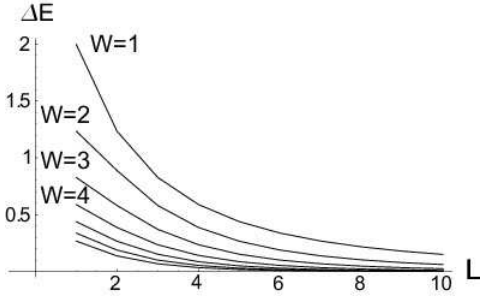


FIG. 4: Band gap of zigzag nanoribbons as a function of length L . The horizontal axes is the length L and the vertical axes is the energy gap ΔE in units of $t = 3\text{eV}$. Each curve is for width $W = 1$ to 7 from top to bottom.

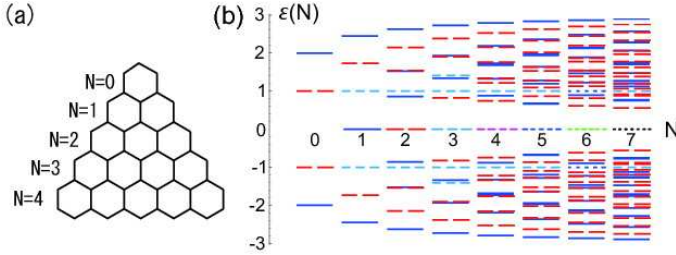


FIG. 5: (Color online) (a) Geometric configuration of trigonal zigzag nanodisks. It is convenient to introduce the size parameter N in this way. The 0-trigonal nanodisk consists of a single Benzene, and so on. The number of carbon atoms are related as $N_C = N^2 + 6N + 6$. See explicit examples given in Fig.7. (b) Density of states of the N -trigonal nanodisk for $N = 0, 1, 2, \dots, 7$. The horizontal axis is the size N and the vertical axis is the energy $\varepsilon(N)$ in units of $t = 3\text{eV}$. Dots on colored bar indicate the degeneracy of energy levels.

with $|n(E)| \leq 1$. We then make the inversion of this formula to derive E as a function of n . See Fig.6 for their correspondence in graphene, where $E(n)$ is found to be a prolonged S-shaped curve.

Diagonalizing the Hamiltonian (2.1) explicitly, we have constructed and displayed $E(n)$ for several nanodisks with trigonal zigzag shape in Fig.7(a), trigonal armchair shape in Fig.7(b) and hexagonal zigzag shape in Fig.7(c). Each diagram consists of step-like segments reflecting the δ -function type density of states (2.2). The length of each step represents the degeneracy of the energy level in units of N_C . It is remarkable that there exist zero-energy states only in trigonal zigzag nanodisks. We have also checked explicitly the absence of the zero-energy state in a series of nanodisks with hexagonal armchair type [Fig.1(e)].

In each figure we have also displayed the prolonged S-shaped curve of graphene, which the $E(n)$ of nanodisk approaches in the large size limit ($N_C \rightarrow \infty$). The prolonged S-shaped curve is universal regardless of the nanodisk's shape.

We investigate trigonal zigzag nanodisks more in details since they have zero-energy states. It can be shown

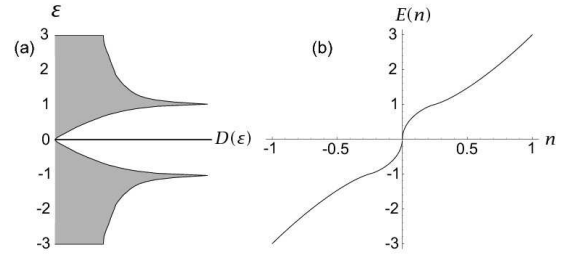


FIG. 6: (a) Density of state $D(\varepsilon)$ as a function of the energy ε in units of $t = 3\text{eV}$ for graphene. (b) The energy $E(n)$ as a function of the doped electron number n . These two functions share the same information of the energy spectrum.

that the determinant associated with the Hamiltonian (2.1) has a factor such that

$$\det[\varepsilon I - H(N_C)] \propto \varepsilon^N (\varepsilon - t)^{a(N)} (\varepsilon + t)^{a(N)}, \quad (3.2)$$

implying the N -fold degeneracy of the zero-energy states and the $a(N)$ -fold degeneracy of the states with the energy $\varepsilon = \pm t$, where

$$a(N) = 3, 3, 3, 3, 3, 5, 3, 5, 3, 7, 3, 7, 3, 9, 3, 9, 3, \dots, \quad (3.3)$$

for $N = 1, 2, 3, \dots$.

Since there exist half-filled zero-energy states for $N \geq 1$, these nanodisks are metallic. The gap energy between the first excitation state and the ground state decreases as the size becomes larger. However, it is remarkable that the gap energy is quite large and is of the order of 3eV even in the nanodisk with size $N = 7$ [Fig.5(b)]. This is much higher than room temperature. Hence, the low-energy physics near the Fermi energy $\varepsilon = 0$ can well be described only by taking the zero-energy states into account.

IV. WAVE FUNCTIONS OF TRIGONAL NANODISKS

A wave function is represented as

$$\varphi(\mathbf{x}) = \sum_i \omega_i \varphi_i(\mathbf{x}), \quad (4.1)$$

where $\varphi_i(\mathbf{x})$ is the Wannier function localized at the lattice point i . The operator c_i in the Hamiltonian (2.1) annihilates an electron in the state described by the Wannier function $\varphi_i(\mathbf{x})$. We are able to calculate the amplitude ω_i for zero-energy states in the trigonal zigzag nanodisk. All of them are found to be real. As an example we show them with size $N = 5$ in Fig.8, where the solid (open) circles denote the amplitude ω_i are positive (negative). The amplitude is proportional to the radius of circle. It is intriguing that one of the wave functions is entirely localized on edge sites for nanodisks with $N = \text{odd}$, as in Fig.8(a). There are no such wave functions for nanodisks with $N = \text{even}$.

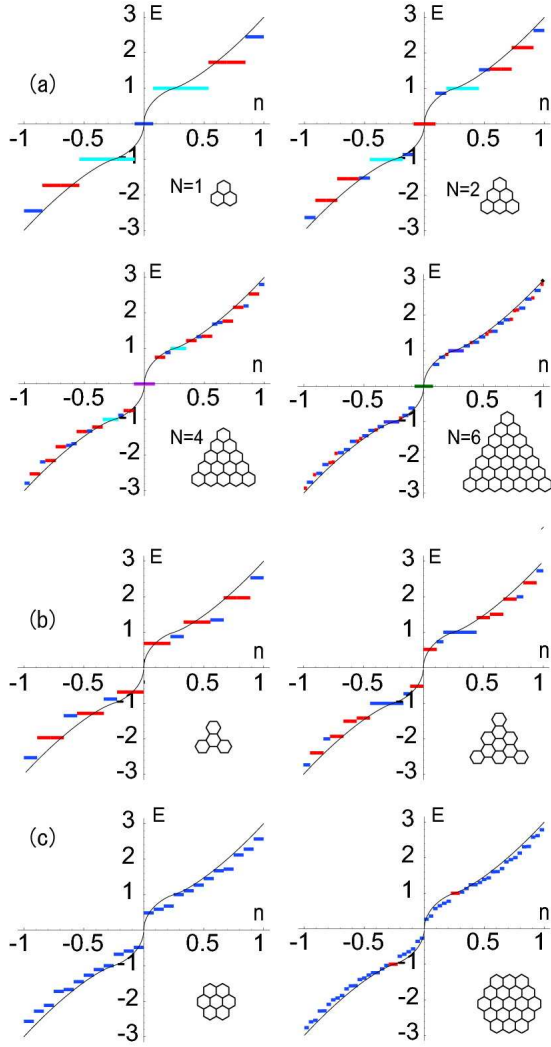


FIG. 7: (Color online) Energy spectrum $E(n)$ as a function of the doped electron number n for (a) trigonal zigzag nanodisks, (b) trigonal armchair nanodisks and (c) hexagonal zigzag nanodisks, with various sizes. The horizontal axis is the number of doped electrons n , and the vertical axis is the energy E in units of $t = 3\text{eV}$. The S-shaped solid curve is that of graphene. The energy density diagrams of nanodisks approach that of graphene for large size. There are degenerate zero-energy states in all trigonal nanodisks, and they are metallic. There are no zero-energy states in all zigzag armchair nanodisks and all hexagonal nanodisks, and they are semiconducting.

The most important property is that all wave functions are nonvanishing on edge sites. In order to demonstrate this, we have investigated how the zero-energy states are modified by changing the site-energy ε_i in the Hamiltonian (2.1) only for edge carbons. Edge carbons are those surrounded by two carbon atoms and one hydrogen atom, while bulk carbons are those surrounded by three carbon atoms⁵. If a wave function vanishes on edges, the zero-energy state must remain as it is. First, we take $\varepsilon_i = \varepsilon - \Delta\varepsilon$ for all edge carbons. We show how the

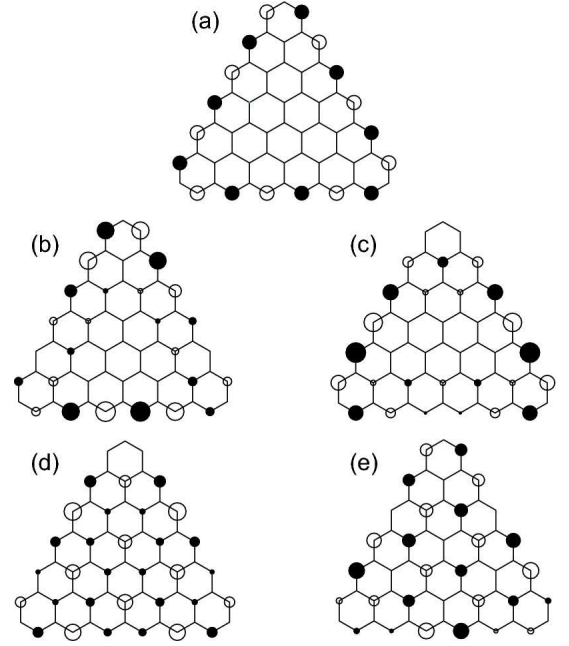


FIG. 8: The zero-energy states of the trigonal nanodisk with size $N = 5$. There are 5 degenerate states, (a) \sim (e). Electrons are localized on edges in the state (a). When the site energy ε_i is decreased at edges equally, the degeneracy is partially resolved, as illustrated in Fig.9(a). The state (a) has the lowest energy and nondegenerate; the states (b) and (c) are degenerate; the states (d) and (e) are degenerate and have the highest energy. When the site energy ε_i is decreased further on the bottom edge, all the degeneracy among these 5 states is resolved, as illustrated in Fig.9(b).

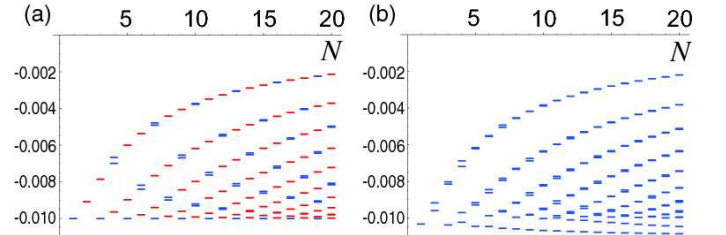


FIG. 9: (Color online) Zero-energy states split into several nonzero-energy states by edge modifications. The horizontal axis is the size N and the vertical axis is the energy in units of $t = 3\text{eV}$. (a) We take $\varepsilon_i = \varepsilon - \Delta\varepsilon$ for all edge carbons with $\Delta\varepsilon = 0.03\text{eV}$. Nonzero-energy states are nondegenerate (blue) or 2-fold degenerate (red). (b) We take $\varepsilon_i = \varepsilon - \Delta\varepsilon - \Delta\varepsilon'$, $\Delta\varepsilon' = 0.003\text{eV}$ for edge carbons on only one of the three edges and $\varepsilon_i = \varepsilon - \Delta\varepsilon$ for those on the other two edges. All states become nondegenerate.

zero-energy states split by taking $\Delta\varepsilon = 0.01t = 0.03\text{eV}$ in Fig.9(a) for $N = 1, 2, \dots, 20$. It is seen that all zero-energy states acquire negative energy and that they become one-fold or two-fold degenerate. The energy decrease is larger when the wave function is localized more on edges. When we decrease the site-energy more, $\varepsilon_i = \varepsilon - \Delta\varepsilon - \Delta\varepsilon'$, $\Delta\varepsilon' = 0.001t = 0.003\text{eV}$ for edge car-

bons on only one of the three edges, all the degeneracy is found to be resolved as in Fig.9(b).

V. MAGNETIC PROPERTIES OF TRIGONAL NANODISKS

We proceed to show that the degenerate ground states lead to a ferromagnetism as in graphene nanoribbon. This is because the Coulomb exchange interaction or the Hund's rule coupling drives all spins to polarize into a single direction. We are most interested how large is the relaxation time for small nanodisks. (Strictly speaking, ferromagnetism can occur only in an infinitely large system, but we may use the terminology for a finite system if the relaxation time is large enough.)

The effective Hamiltonian for the Coulomb exchange interaction is given by the Heisenberg model. Here, for the sake of simplicity, we use the Ising model,

$$H = - \sum_{i \neq j}^N J_{ij} \sigma_i \sigma_j, \quad (5.1)$$

since the Heisenberg model presents essentially the same result on the relaxation time as we shall argue later. In the effective Hamiltonian, σ_i is the spin operators of electrons in the i th zero-energy state, $\sigma_i = \pm 1$, and the summation is taken over all electron pairs. An important point is that the exchange interaction strength J_{ij} must be nonzero for all electron pairs because their wave functions are nonvanishing on edges. This is in a sharp contrast to the Hamiltonian for a nanomagnet, where J_{ij} can be regarded nonvanishing only for neighboring electron pairs since the index i represents the site in the real space. This makes a clear difference in the relaxation time as we shall soon see.

The spin dynamics is well described by the master equation, $dP(t)/dt = \mathcal{L}P(t)$, where the symbol P denotes the probability distribution function specifying the spin configuration, and \mathcal{L} is the Liouville operator associated with the Hamiltonian. When the expansion $P(0) = \sum_{\lambda} c_{\lambda} P_{\lambda}$ holds at the initial state at time $t = 0$, the state of the system at any later time is given by

$$P(t) = e^{\mathcal{L}t} P(0) = \sum_{\lambda} c_{\lambda} e^{-\lambda t} P_{\lambda}, \quad (5.2)$$

where λ is obtained by solving the eigenvalue equation, $\mathcal{L}P_{\lambda} = -\lambda P_{\lambda}$. The relaxation rate of the system is equal to the minimum eigenvalue λ_{\min} of the Liouville operator. Thus the relaxation time is given by $\tau = 1/\lambda_{\min}$.

To get a concrete idea, since all J_{ij} are nonvanishing, we first make an estimation by making an approximation $J_{ij} = J$. We are able to diagonalize the Ising Hamiltonian (5.1) explicitly. The eigenvalues are given by

$$E_n = -\frac{J}{2} [(N - 2n)^2 - N], \quad (5.3)$$

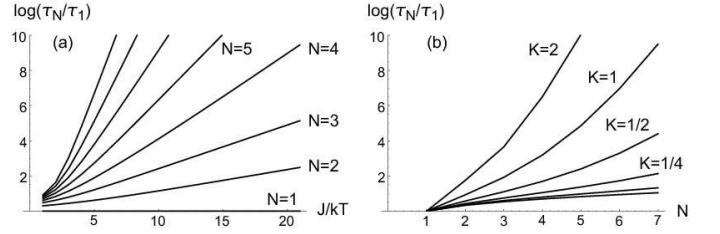


FIG. 10: Relaxation time of various graphene nanodisks. (a) The relaxation time of nanodisks with size $N = 1, 2, \dots, 8$ from bottom to top. The horizontal axis is the coupling constant J/kT and the vertical axis is the relaxation time in the form of $\log_{10}[\tau_N/\tau_1]$. (b) The relaxation time of nanodisks with interaction strength $K \equiv J/kT = 1/16, 1/8, 1/4, 1/2, 1, 2$ from bottom to top. The horizontal axis is the size of nanodisks N .

where $n = 0, 1, 2, \dots, N$ is the energy level index. We have then carried out an exact diagonalization of the eigenvalue problem of the Liouville operator \mathcal{L} and determined the eigenvalue λ_{\min} . We show the relaxation time as a function of the coupling strength J/kT for various size N in Fig.10(a) and as a function of size for various coupling strength in Fig.10(b).

For the noninteracting case, $J/kT = 0$, it is easy to see that the relaxation time τ_N of the N -trigonal zigzag nanodisk is given by

$$\tau_N = N\tau_1.$$

On the other hand, the relaxation rate λ_{\min} is given by the Arrhenius-type formula for strong coupling limit or in low temperature limit, $J/kT \gg 1$. Hence the relaxation time is given by

$$\tau_N = \exp\left[\frac{\Delta E}{kT}\right] \tau_1, \quad (5.4)$$

where

$$\begin{aligned} \Delta E &= JN^2/2 & \text{for } N = \text{even}, \\ \Delta E &= J(N^2 - 1)/2 & \text{for } N = \text{odd} \end{aligned} \quad (5.5)$$

is the energy difference between the highest energy state and the ground state. It is observed in Fig.10 that the relaxation time is given by the asymptotic formula (5.4) already for $J \gtrsim kT$.

The relaxation rate is given by the Arrhenius-type formula also in the generic model (5.1) with $J_{ij} \neq J$, where ΔE is the energy difference between the highest energy state and the ground state. Then, the relaxation time is given by (5.4) by replacing J with

$$J_{\text{eff}} \simeq \frac{1}{N(N-1)} \sum_{i \neq j}^N J_{ij}, \quad (5.6)$$

which is of the order of a typical J_{ij} . Furthermore, we would obtain the same result for the Heisenberg model even with $J_{ij} \neq J$.

Note that in an ordinary nanomagnet composed of N spins, the relaxation time is given by (5.4) with

$$\Delta E = JNz, \quad (5.7)$$

where z is the number of the nearest neighboring spins. It is remarkable that the size dependence of the relaxation time is $\propto N^2$ for trigonal zigzag nanodisks, though it is $\propto N$ for normal nanomagnets. This is because any one spin couples with all other spins in the zero-energy state.

VI. DISCUSSIONS

Graphene derivatives become metallic when they have half-filled zero-energy states. We have explored the energy spectra in a wide class of nanodisks as well as finite-length nanoribbons. It is surprising that the emergence of zero-energy states is quite rare. There exist no zero-energy states in finite-length zigzag nanoribbons. However, the band gap decreases inversely to the length, and zero-energy states emerge as $L \rightarrow \infty$. Hence, a sufficiently long nanoribbon can be regarded practically as a metal.

Among a wide class of nanodisks we have studied, trigonal zigzag nanodisks are distinguished for their elec-

tronic properties since they exhibit metallic ferromagnetism due to their half-filled degenerate zero-energy states. The degeneracy is controllable arbitrarily by changing the size of nanodisks. We have estimated the relaxation time, which has been argued to be proportional to $\exp[J_{\text{eff}}N^2/2kT]$ when the size is N . Though the numerical estimation of the effective spin stiffness J_{eff} is yet to be done, it is of the order of the Coulomb energy since its origin is the exchange interaction or the Hund's coupling rule. We conclude that the relaxation time is quite large for its size at low temperature $T \lesssim J_{\text{eff}}/2k$. Hence, for instance, it could be used as a memory device. By connecting nanodisks with nanoribbons, we can design electronic circuits. These devices would be obtained by etching a single graphene. Alternatively, nanodisks may be connected with leads by making tunneling junctions. We would like to make an analysis of the nanodisk and lead system together with related phenomena in future works.

I am very much grateful to Professors Y. Hirayama and K. Hashimoto for many fruitful discussions on the subject. The work was in part supported by Grants-in-Aid for Scientific Research from Ministry of Education, Science, Sports and Culture (Nos.070500000466).

-
- ¹ K.S. Novoselov, A.K. Geim, S.V. Morozov, D. Jiang, Y. Zhang, S.V. Dubonos, I.V. Grigorieva, and A.A. Firsov, *Science* **306**, 666 (2004).
 - ² K.S. Novoselov, A.K. Geim, S.V. Morozov, D. Jiang, M.I. Katsnelson, I.V. Grigorieva, S.V. Dubonos, and A.A. Firsov, *Nature* **438**, 197 (2005).
 - ³ Y. Zhang, Y-W Tan, H.L. Stormer, and P. Kim, *Nature* **438**, 201 (2005).
 - ⁴ M. Fujita, K. Wakabayashi, K. Nakada, and K. Kusakabe, *J. Phys. Soc. Jpn.* **65**, 1920 (1996).
 - ⁵ M. Ezawa, *Phys. Rev. B*, **73**, 045432 (2006).
 - ⁶ L. Brey, and H.A. Fertig, *Phys. Rev. B*, **73**, 235411 (2006); L. Brey, and H.A. Fertig, *Phys. Rev. B*, **75** 125434 (2007).
 - ⁷ F. Muñoz-Rojas, D. Jacob, J. Fernández-Rossier, and J. J. Palacios, *Phys. Rev. B*, **74**, 195417 (2006).
 - ⁸ Y-W Son, M.L. Cohen, and S.G. Louie, *Phys. Rev. Lett.*, **97**, 216803 (2006); Y-W Son, M.L. Cohen, and S.G. Louie, *Nature*, **444**, 347 (2006).
 - ⁹ V. Barone, O. Hod, and G.E. Scuseria, *Nano Lett.*, **6**, 2748 (2006).
 - ¹⁰ M.Y. Han, B. Oezylmaz, Y. Zhang, and P. Kim, *Phys. Rev. Lett.*, **98**, 206805 (2007).
 - ¹¹ Z. Chen, Y-M. Lin, M.J. Rooks, and P. Avouris, *cond-mat/0701599*.
 - ¹² Z. Xu and Q-S. Zheng, *Appl. Phys. Lett.* **90**, 223115 (2007).
 - ¹³ C. Berger, Z. Song, X. Li, X. Wu, N. Brown, C. Naud, D. Mayou, T. Li, J. Hass, A.N. Marchenkov, E.H. Conrad, P.N. First and W.A. de Heer, *Science* **312**, 119 (2006).
 - ¹⁴ M. Ezawa, *Physica Status Solidi (c)* **4**, No.2, 489 (2007).
 - ¹⁵ H.J. Räder, A. Rouhanipour, A.M. Talarico, V. Palermo, P. Samorì, and K. Müllen, *Nature materials* **5**, 276 (2006).
 - ¹⁶ R. Saito, G. Dresselhaus, and M. S. Dresselhaus, *Physical Properties of Carbon Nanotubes*, Imperial College Press, 1998, London.